Statical and dynamical structural analysis by a kinematical description of the small strains involving finite rotations

S. Lopez[1], G. La Sala
Dipartimento di Modellistica per l'Ingegneria, Universit della Calabria, 87030 Rende, Italy
[1] *E-mail: salvatore.lopez@unical.it*

Keywords: statical and dynamical structural analysis; small strains - finite rotations; selective strain definitions

SUMMARY. A geometrically nonlinear formulation to analyse structures in the hypotheses of large displacements and rotations and small strains is presented. In this formulation, applied to low-order elements and based on the total Lagrangian kinematics, the use of the rotation matrices is bypassed. A selective based definition of the strain tensor, used in order to avoid shear-locking problems, is effected by the linear definition of deformations because it is element reference system independent. In addition, complex manipulations required to obtain conservative descriptions and well-posed transformation matrices are avoided. Numerical tests have been carried out to evaluate the validity of the developed technique both in the statical and in the dynamical context.

1 INTRODUCTION

In the geometrically nonlinear structural mechanics context, a considerable work has been developing on the formulation of models, for two or three-dimensional elastic structures, in the case of small strains in the large displacements regime. Large-scale calculations required by these formulations have encouraged the adoption of simpler and faster elements and of more efficient treatements of the finite rotations. Tipically, definitions of lower-order quadrilateral or hexahedral isoparametric elements are the most adapted provided that we overcome the connected locking problems in the cases of thin structures.

In this context, classically a corotational approach is used. The motion of the continuous medium is decomposed into a rigid body motion followed by a pure deformation. For this reason, the finite element is studied in the linear case where the drawback, due to the locking phenomena, clearly appears. Afterward, the nonlinear motion is obtained by joining the linear kinematic with a rigid body motion that is recovered by use of orthogonal transformation matrices. The evolution of the corotational approach can be traced by referring to the significant works of Belytschko and Hsieh [1], Rankin and Nour-Omid [2] and Pacoste [3].

In a potential energy based approach, initial responses to the locking problem have led to the selective integration techniques. They are based on a split of the strain energy into individual parts on which different integration rules in the evaluation of corresponding contributions in the stiffness matrix are applied (Zienkiewicz et al. [4]). A good response to instability problems, due to the probable presence of energy zero modes, has been the reduced integration method with hourglass control introduced by Kosloff and Frazier [5], then developed with better computational performances by Flanagan and Belytschko [6].

These techniques, however, have to be supported by an adapted, robust and economical definition of the rotated local reference system. The choice of this reference system, anyhow, affects the features obtained for the studied element in the linear assumptions. Basically, moreover, the corotational approach suffers from the singularities in the transformation matrices for several angles and requires complex manipulations to overcome nonconservative descriptions due to the noncommutativity of rotations.

In this paper we present a small strains - finite displacements description by a potential energy based finite element formulation where the use of rotation matrices is avoided. The described technique preserves the possibility to study the finite element in the linear field and retains the analysis robust and economical.

Generically, to draw out from the complete nonlinear strain tensor only the contributes due to the deformations is a problematic process. Closed forms of the deformative expressions are difficultly definible also in the case of extraction of the linear contributes. In effect, the Lagrangian finite strain tensor implicitly considers at the same time both the nonlinearities due to the rigid and deformative motions. In our context, the actual configuration of the element results rigidly translated and rotated and deformed according to the selected linear modes. The aim is to found, for each deformative mode, a characteristic measure that is an invariant to the rotations. In such a way the linear deformation modes become reciprocally independent and then they can be summed up in the strain tensor definition. The invariant measures have been computed, then, by requiring for each of them the following two features: not zero for the examined deformative mode and equal to zero for the other modes in the initial configuration; independent of the rigid kinematics value.

2 LINEAR KINEMATICAL BASIS IN THE 4-NODE AND 8-NODE ELEMENTS

In regard to the two-dimensional element we refer to the bilinear rectangular $2h_\xi$, $2h_\eta$ 4-node element centered in the origin $O = (0, 0)$ of the (ξ, η) reference system (see Figure 1). The strains obtained from this interpolation can be expressed into a basis of the three rigid and of five deformative motions. These latter are shown in Figure 2.

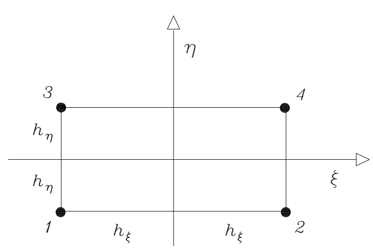

Figure 1: Two-dimensional 4-node element: definition.

Similarly, for the three-dimensional element we refer now to the trilinear $2h_\xi$, $2h_\eta$, $2h_\zeta$ 8-node element still centered in the origin $O = (0, 0, 0)$ of the (ξ, η, ζ) reference system (see Figure 3). The consequently strains are referred to the basis of the six rigid and eighteen deformative motions. Representations of these modes are shown in the Figures 4-8.

3 DEFORMATIVE INVARIANTS DEFINITIONS

3.1 Regular geometries

We consider a generic configuration of the element. This configuration, therefore, results rigidly translated, rotated and deformed according to the modes described in the previous section. Now, for each deformative mode, we identify a measure with the following two features: not zero for the examined mode and equal to zero for the other modes in the initial configuration; independent of

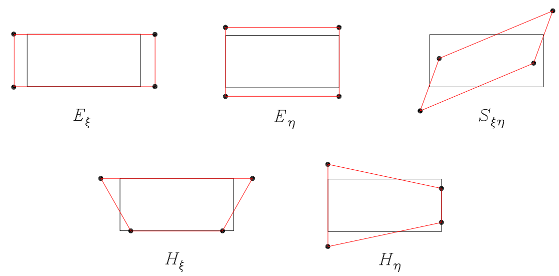

Figure 2: Four-node element: representations of the linear deformative modes.

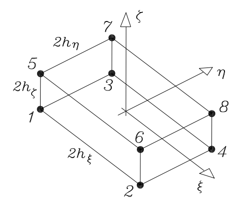

Figure 3: Three-dimensional 8-node element: definition.

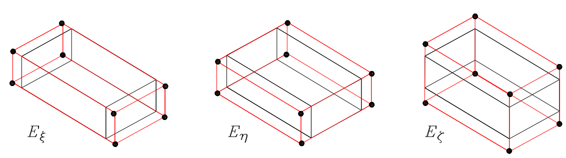

Figure 4: Eight-node element: representations of the expansion modes.

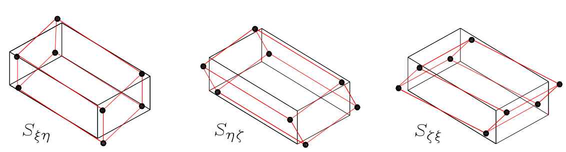

Figure 5: Eight-node element: representations of the shearing modes.

the rigid kinematics value. Then, such a measure univocally describes the deformation associated with the mode itself in the generic configuration. So, these definitions make the deformative modes reciprocally independent and then, they can be summed up in the strain tensor definitions.

The measures just described, denoted in the following as deformative invariants, represent here relative distances between points of the generic configuration and they are in function of the unknown elemental parameters. As distances we refer to the Euclidean measure $\mathcal{D}(p_i, p_j)$ between the points p_i, p_j of the element in the generic configuration:

$$\mathcal{D}(p_i, p_j) = \sqrt{\left[\xi_i^p + u_i^p - \xi_j^p - u_j^p\right]^2 + \left[\eta_i^p + v_i^p - \eta_j^p - v_j^p\right]^2 + \left[\zeta_i^p + w_i^p - \zeta_j^p - w_j^p\right]^2}. \quad (1)$$

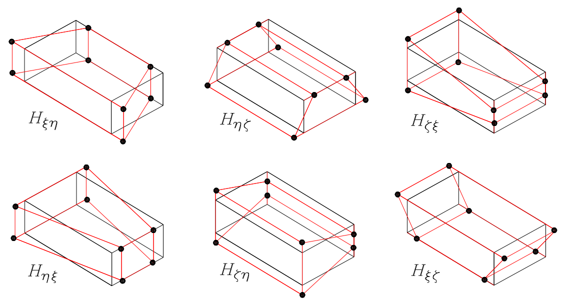

Figure 6: Eight-node element: representations of the hourglass modes.

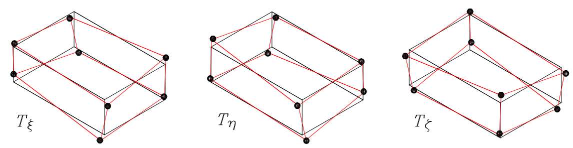

Figure 7: Eight-node element: representations of the torsional modes.

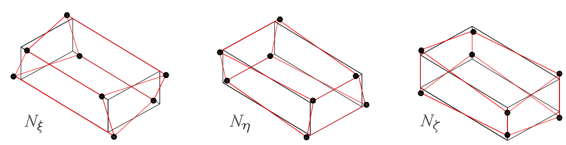

Figure 8: Eight-node element: representations of the non-physical modes.

In (1) ξ_i^p, η_i^p and ζ_i^p are, respectively, the initial ξ, η and ζ coordinates of the point p_i while u_i^p, v_i^p and w_i^p are the respective displacements.

As an example, we refer to the two-dimensional ξ extensional mode. We describe how to define the related characteristic measure and that it represents an invariant in respect to the deformation fields. We consider (refer to the Figure 1) the distance $\mathcal{D}(p_{13}, p_{24})$ between the middle points m_{13} and m_{24} of the segments n_1-n_3 and n_2-n_4 connecting the n_i nodes of the element. We note that this distance is an invariant, in the first order approximation, in respect to the remaining η extensional, shearing, ξ and η hourglass modes as shown in Figures 9(a), 9(b), 9(c) and 9(d), respectively. As we can verify, the examined $\mathcal{D}(m_{13}, m_{24})$ distance changes only if the actual configuration of the element involves also the ξ extensional deformation (see Figure 9(e)).

Then, a possible choice for the invariant $\mathcal{I}E_\xi$ related to the deformative parameter E_ξ is:

$$\mathcal{I}E_\xi = \mathcal{D}(m_{13}, m_{24}) - 2h_\xi. \tag{2}$$

This invariant, therefore, represents the difference between the actual $\mathcal{D}(m_{13}, m_{24})$ and the initial $2h_\xi$ distances. Of course, this difference is equal to the ξ expansion of the element. So, the following relation is valid:

$$\mathcal{I}E_\xi = 2E_\xi h_\xi. \tag{3}$$

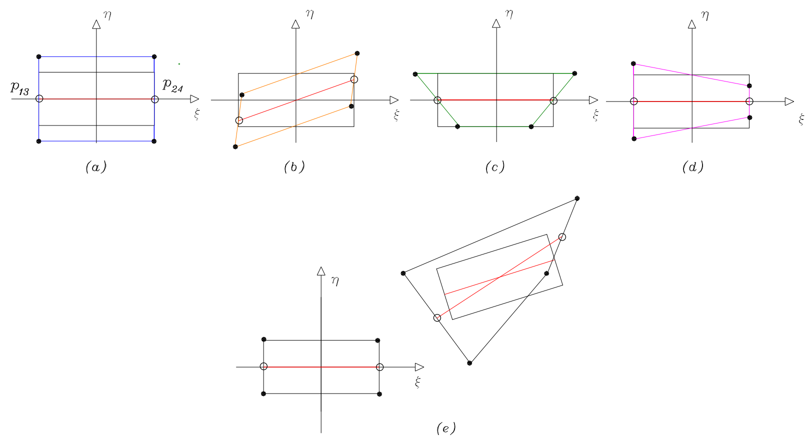

Figure 9: Two-dimensional 4-node element: examination of the $\mathcal{I}E_\xi$ invariant.

In the following we define the invariants by basing our measures only on nodal distances. In Table 1 for the two-dimensional case and in Tables 2-6 for the three-dimensional case, the used definitions of the invariants and their dependence on the related deformative parameters are given .

$\mathcal{I}E_\xi = (\mathcal{D}(n_1,n_2)+\mathcal{D}(n_3,n_4))/2 - 2h_\xi$	$E_\xi = \mathcal{I}E_\xi/2h_\xi$
$\mathcal{I}E_\eta = (\mathcal{D}(n_1,n_3)+\mathcal{D}(n_2,n_4))/2 - 2h_\eta$	$E_\eta = \mathcal{I}E_\eta/2h_\eta$
$\mathcal{I}S_{\xi\eta} = \mathcal{D}(n_1,n_4) - \mathcal{D}(n_2,n_3)$	$S_{\xi\eta} = \mathcal{I}S_{\xi\eta}\sqrt{(h_\xi)^2+(h_\eta)^2}/8h_\eta h_\xi$
$\mathcal{I}H_\xi = \mathcal{D}(n_1,n_2) - \mathcal{D}(n_3,n_4)$	$H_\xi = \mathcal{I}H_\xi/4h_\xi h_\eta$
$\mathcal{I}H_\eta = \mathcal{D}(n_1,n_3) - \mathcal{D}(n_2,n_4)$	$H_\eta = \mathcal{I}H_\eta/4h_\eta h_\xi$

Table 1: Deformations of the 4-node element: invariants and parameters expressions.

$\mathcal{I}E_\xi = (\mathcal{D}(n_1,n_2)+\mathcal{D}(n_3,n_4)+\mathcal{D}(n_5,n_6)+\mathcal{D}(n_7,n_8))/4 - 2h_\xi$	$E_\xi = \mathcal{I}E_\xi/2h_\xi$
$\mathcal{I}E_\eta = (\mathcal{D}(n_1,n_3)+\mathcal{D}(n_2,n_4)+\mathcal{D}(n_5,n_7)+\mathcal{D}(n_6,n_8))/4 - 2h_\eta$	$E_\eta = \mathcal{I}E_\eta/2h_\eta$
$\mathcal{I}E_\zeta = (\mathcal{D}(n_1,n_5)+\mathcal{D}(n_2,n_6)+\mathcal{D}(n_3,n_7)+\mathcal{D}(n_4,n_8))/4 - 2h_\zeta$	$E_\zeta = \mathcal{I}E_\zeta/2h_\zeta$

Table 2: Extensions of the 8-node element: invariants and parameters expressions.

$\mathcal{I}S_{\xi\eta} = \mathcal{D}(n_1,n_4)+\mathcal{D}(n_5,n_8)-\mathcal{D}(n_2,n_3)-\mathcal{D}(n_6,n_7)$	$S_{\xi\eta} = \mathcal{I}S_{\xi\eta}\sqrt{(h_\xi)^2+(h_\eta)^2}/16h_\xi h_\eta$
$\mathcal{I}S_{\eta\zeta} = \mathcal{D}(n_2,n_8)+\mathcal{D}(n_1,n_7)-\mathcal{D}(n_4,n_6)-\mathcal{D}(n_3,n_5)$	$S_{\eta\zeta} = \mathcal{I}S_{\eta\zeta}\sqrt{(h_\eta)^2+(h_\zeta)^2}/16h_\eta h_\zeta$
$\mathcal{I}S_{\zeta\xi} = \mathcal{D}(n_1,n_6)+\mathcal{D}(n_3,n_8)-\mathcal{D}(n_2,n_5)-\mathcal{D}(n_4,n_7)$	$S_{\zeta\xi} = \mathcal{I}S_{\zeta\xi}\sqrt{(h_\xi)^2+(h_\zeta)^2}/16h_\xi h_\zeta$

Table 3: Shearings of the 8-node element: invariants and parameters expressions.

3.2 Distorted geometries

For generic quadrilateral and hexahedral elements, we refer to the same measures of the invariants given in the previously section. This assumption, however, is consistent if the invariant definition requirements are satisfied. So, in respect to the invariants individuation of the previous section carried out by inspection of the modes, it is possible to proceed in such a way that the requirements are satisfied in a constructive manner, that is adopting a related general inverse procedure.

$\mathcal{I}H_{\xi\eta} = \mathcal{D}(n_3, n_4) + \mathcal{D}(n_7, n_8) - \mathcal{D}(n_1, n_2) - \mathcal{D}(n_5, n_6)$	$H_{\xi\eta} = \mathcal{I}H_{\xi\eta}/8h_\xi h_\eta$
$\mathcal{I}H_{\eta\zeta} = \mathcal{D}(n_5, n_7) + \mathcal{D}(n_6, n_8) - \mathcal{D}(n_1, n_3) - \mathcal{D}(n_2, n_4)$	$H_{\eta\zeta} = \mathcal{I}H_{\eta\zeta}/8h_\eta h_\zeta$
$\mathcal{I}H_{\zeta\xi} = \mathcal{D}(n_2, n_6) + \mathcal{D}(n_4, n_8) - \mathcal{D}(n_1, n_5) - \mathcal{D}(n_3, n_7)$	$H_{\zeta\xi} = \mathcal{I}H_{\zeta\xi}/8h_\xi h_\zeta$
$\mathcal{I}H_{\eta\xi} = \mathcal{D}(n_2, n_4) + \mathcal{D}(n_6, n_8) - \mathcal{D}(n_1, n_3) - \mathcal{D}(n_5, n_7)$	$H_{\eta\xi} = \mathcal{I}H_{\eta\xi}/8h_\xi h_\eta$
$\mathcal{I}H_{\zeta\eta} = \mathcal{D}(n_3, n_7) + \mathcal{D}(n_4, n_8) - \mathcal{D}(n_1, n_5) - \mathcal{D}(n_2, n_6)$	$H_{\zeta\eta} = \mathcal{I}H_{\zeta\eta}/8h_\eta h_\zeta$
$\mathcal{I}H_{\xi\zeta} = \mathcal{D}(n_5, n_6) + \mathcal{D}(n_7, n_8) - \mathcal{D}(n_1, n_2) - \mathcal{D}(n_3, n_4)$	$H_{\xi\zeta} = \mathcal{I}H_{\xi\zeta}/8h_\xi h_\zeta$

Table 4: Hourglass of the 8-node element: invariants and parameters expressions.

$\mathcal{I}T_\zeta = \mathcal{D}(n_2, n_3) + \mathcal{D}(n_5, n_8) - \mathcal{D}(n_1, n_4) - \mathcal{D}(n_6, n_7)$	$T_\zeta = \mathcal{I}T_\zeta\sqrt{(h_\xi)^2 + (h_\eta)^2)}/16h_\xi h_\eta h_\zeta$
$\mathcal{I}T_\eta = \mathcal{D}(n_2, n_5) + \mathcal{D}(n_3, n_8) - \mathcal{D}(n_1, n_6) - \mathcal{D}(n_4, n_7)$	$T_\eta = \mathcal{I}T_\eta\sqrt{(h_\xi)^2 + (h_\zeta)^2}/16h_\xi h_\eta h_\zeta$
$\mathcal{I}T_\xi = \mathcal{D}(n_2, n_8) + \mathcal{D}(n_3, n_5) - \mathcal{D}(n_1, n_7) - \mathcal{D}(n_4, n_6)$	$T_\xi = \mathcal{I}T_\xi\sqrt{(h_\eta)^2 + (h_\zeta)^2}/16h_\xi h_\eta h_\zeta$

Table 5: Torsions of the 8-node element: invariants and parameters expressions.

$\mathcal{I}N_\xi = \mathcal{D}(n_1, n_2) + \mathcal{D}(n_7, n_8) - \mathcal{D}(n_3, n_4) - \mathcal{D}(n_5, n_6)$	$N_\xi = \mathcal{I}N_\xi/8h_\xi h_\eta h_\zeta$
$\mathcal{I}N_\eta = \mathcal{D}(n_1, n_3) + \mathcal{D}(n_6, n_8) - \mathcal{D}(n_2, n_4) - \mathcal{D}(n_5, n_7)$	$N_\eta = \mathcal{I}N_\eta/8h_\xi h_\eta h_\zeta$
$\mathcal{I}N_\zeta = \mathcal{D}(n_1, n_5) + \mathcal{D}(n_4, n_8) - \mathcal{D}(n_2, n_6) - \mathcal{D}(n_3, n_7)$	$N_\zeta = \mathcal{I}N_\zeta/8h_\xi h_\eta h_\zeta$

Table 6: Non-physical deformations of the 8-node element: invariants and parameters expressions.

In fact, the expressions of the invariants can be defined a priori as a function of the nodal displacements. To compute these unknown displacements, we define a linear algebraic system for each invariant. The equations of the linear system are obtained by imposing zero values for all invariant expressions except the value of the considered one. In this way, by also constraining the rigid motions of the element, the kinematics related to the invariant mode is complitely determined by the computed nodal displacements. In this sense, the approch proves to be systematic and it acquires generality in the isoparametric element field.

4 GEOMETRICALLY NONLINEAR STATICAL AND DYNAMICAL ANALYSIS

The energetic quantities involved in the statical analysis are the $V(\mathbf{u})$ internal potential and the $L(\mathbf{u})$ external work to which we have to add the kinetic energy $T(\dot{\mathbf{u}})$ in the dynamical case.

We focus, now, on the description of the strain tensor in internal potential. We refer to the linear approximation of the tensor components, being, as above-mentioned, the geometrical nonlinearity taken in to account by the definition of the deformative invariants. The tensor, then, is expressed as a linear function of the deformative parameters:

$$\left\{ \begin{array}{l} \varepsilon_{\xi\xi} = \varepsilon_{\xi\xi}(E_\xi, E_\eta, H_\xi, H_\eta) \\ \varepsilon_{\xi\eta} = \varepsilon_{\xi\eta}(S_{\xi\eta}) \\ \varepsilon_{\eta\eta} = \varepsilon_{\eta\eta}(E_\xi, E_\eta, H_\xi, H_\eta) \end{array} \right. \tag{4}$$

for the two-dimensional case, while

$$\begin{cases} \varepsilon_{\xi\xi} = \varepsilon_{\xi\xi}(E_\xi, E_\eta, E_\zeta, H_{\xi\eta}, H_{\eta\zeta}, H_{\zeta\xi}, H_{\eta\xi}, H_{\zeta\eta}, H_{\xi\zeta}, N_\xi, N_\eta, N_\zeta) \\ \varepsilon_{\xi\eta} = \varepsilon_{\xi\eta}(S_{\xi\eta}, S_{\eta\zeta}, S_{\zeta\xi}, T_\xi, T_\eta, T_\zeta) \\ \varepsilon_{\xi\zeta} = \varepsilon_{\xi\zeta}(S_{\xi\eta}, S_{\eta\zeta}, S_{\zeta\xi}, T_\xi, T_\eta, T_\zeta) \\ \varepsilon_{\eta\eta} = \varepsilon_{\eta\eta}(E_\xi, E_\eta, E_\zeta, H_{\xi\eta}, H_{\eta\zeta}, H_{\zeta\xi}, H_{\eta\xi}, H_{\zeta\eta}, H_{\xi\zeta}, N_\xi, N_\eta, N_\zeta) \\ \varepsilon_{\eta\zeta} = \varepsilon_{\eta\zeta}(S_{\xi\eta}, S_{\eta\zeta}, S_{\zeta\xi}, T_\xi, T_\eta, T_\zeta) \\ \varepsilon_{\zeta\zeta} = \varepsilon_{\zeta\zeta}(E_\xi, E_\eta, E_\zeta, H_{\xi\eta}, H_{\eta\zeta}, H_{\zeta\xi}, H_{\eta\xi}, H_{\zeta\eta}, H_{\xi\zeta}, N_\xi, N_\eta, N_\zeta) \end{cases} \tag{5}$$

for the three-dimensional case. Locking effects are overcome by a selective choice of the modes in the (4) and (5) expressions. This selective reduction of the strain components, as said before, can be carried out by a simple zeroing of the undesired deformative parameters. In particular, in (4) and (5) we have omitted the shearing and torsional terms in the normal strain components while extension, hourglass and non-physical modes have been cancelled in the shear strain components.

The potential V, then, results defined by the deformative parameters that are in function of the unknown nodal displacements. As we said, by chain rule we can compute the element internal forces vector and stiffness matrix. The computational cost required by the storage and evalutation of this vectorial quantities results small. In effect, we observe that this is about equal to one-third of the computational cost required by the formulation with classical nonlinear deformations tensor.

The energetic quantities definition allows the formulation of the internal and the external forces to define the statical equilibrium equation and also of the inertial force to define the semidiscrete formulation of the equations of the motion.

A predictor-corrector scheme as described in [7]-[8] for the equilibrium path individualization is used in the statical analysis. It is characterized by a predictor step obtained by an asymptotic extrapolation and by a corrector scheme Newton's method based with minimization of the distance between approximate and equilibrium points as a constraint equation. For the time-integration scheme of the initial value problem we use the Newmark average acceleration method.

5 NUMERICAL EXAMPLES

A set of examples is examined to illustrate the features of the presented formulation. In particular, the tests analyze plane and spatial kinematics by modelling the body with the described two and three-dimensional elements.

5.1 Deep circular arch under vertical load

Equilibrium states for the deep circular arch were computed by the two-dimensional finite element formulation. Several authors, Simo and Vu-Quoc [9], Cardona and Huespe [10], have analyzed the equilibrium paths for such a structure by using one-dimensional finite element in the geometrically nonlinear regime. A 32 equally-spaced element mesh for the whole arch is employed.

We note that, to compare the results, simple support boundary condition requires a proper treatment because quadrilateral two-dimensional elements are used. In particular, here Lagrangian multipliers are adopted to impose zero values for the displacements at the central point of the elemental edge and for the related nodal internal forces.

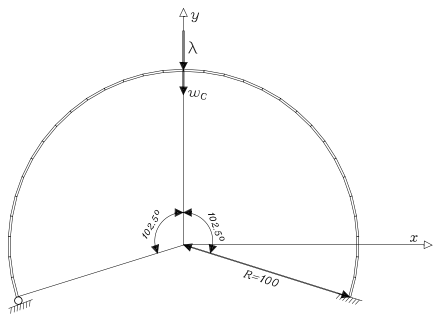

Young's modulus $E = 6 \times 10^6$
Poisson's ratio $\nu = 0.$
Normal area squared with edge equal to $\sqrt{2}$.
Mass density $\rho = 0.0025$
Load history $\lambda = 25t$

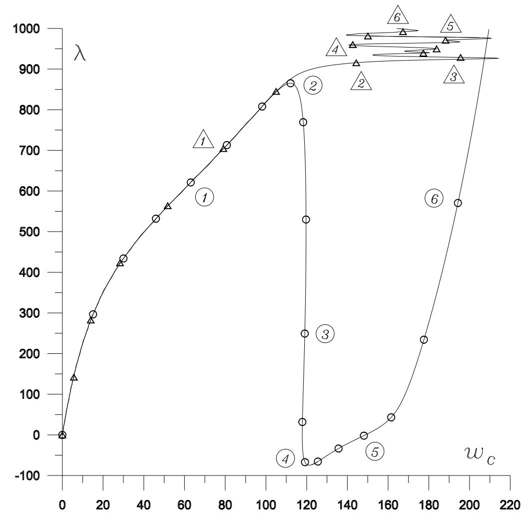

The $\lambda - w_c$ vertical load parameter - deflection of the apex curve was computed for both the statical and dynamical analysis. The analyses are stopped when the value $\lambda = 1000$ is traversing. For the statical case, the graphed primary path shows a good agreement with the results reported in the cited literature. For the dynamical case, the modejump at the first limit point can be observed in the same figure. Deformed configurations of the structure at the marked equilibrium points are depicted in Figure 10 both for the statical and the dinamical case.

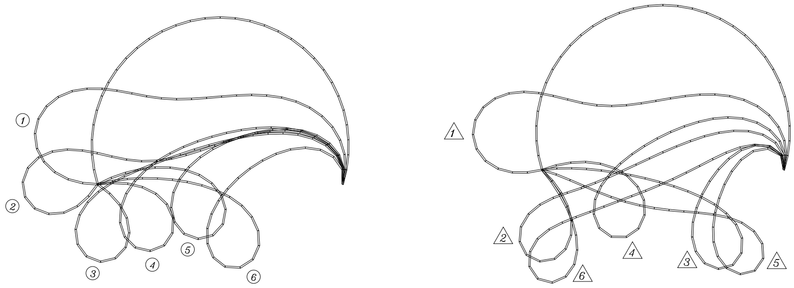

Figure 10: Deep arch: statical and dynamical deformative configurations at marked solution points.

5.2 Nonlinear cylindrical shell

A cylindrical shell of constant thickness and deformed by an applied compressive load is analysed. In this example, studied in Eriksson [11] by two-dimensional thin shell elements we consider vanishing radial and tangential displacements on both ends. A 8×8 mesh for the symmetric quarter of the shell was considered. Then, $v = 0$ for the nodes along the symmetric circumferential edge and $u = 0$ for the nodes along the symmetric longitudinal edge. As before, proper treatment of the central points of the elemental edge at boundaries is carried out. Load parameter λ - central point deflection w_c behaviour for both the statical and dynamical solutions when the algorithm is stopped for the achieved $\lambda = 800$ value are showed.

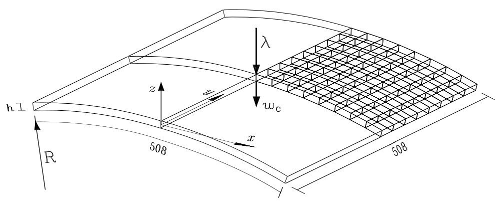

Young's modulus $E = 63103$
Poisson's ratio $\nu = 0.3$
Radius $R = 2540$
Thickness $h = 6.35$
Mass density $\rho = 1$
Load history $\lambda = 0.1t$

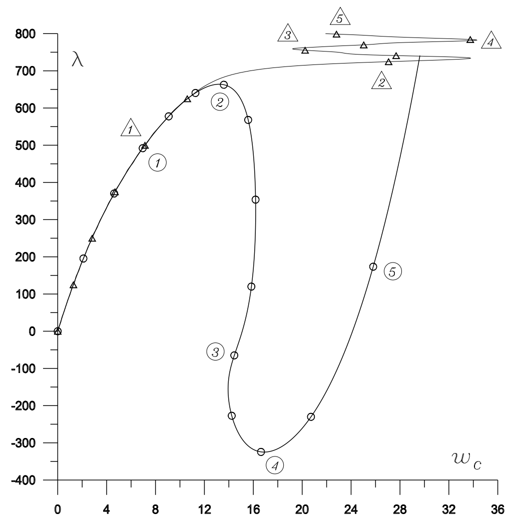

For the statical analysis, deformations in the pre and post-critical phase are displayed in Figure 11. Post modejumping deformations are also shown in Figure 12 for the related dynamical model.

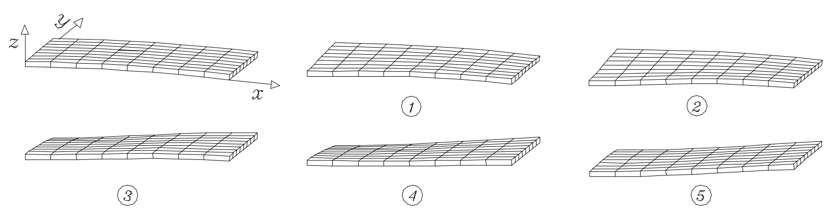

Figure 11: Cylindrical shell: statical deformative configurations at marked solution points.

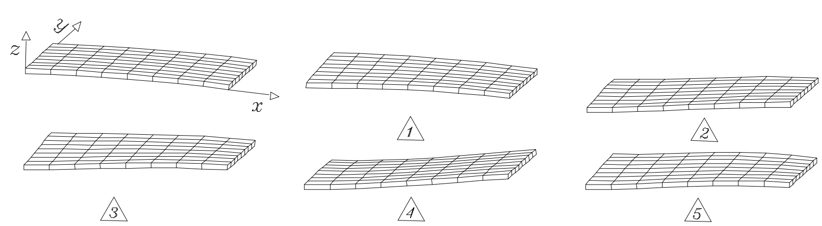

Figure 12: Cylindrical shell: dynamical deformative configurations at marked solution points.

6 CONCLUSIONS

A technique to analyse the motion of structures in the case of large displacements and rotations and small strains has been presented. The described formulation is applied to low-order elements and it does not use rotation measures. In order to avoid shear-locking phenomena, a selective based definition of the strain tensor is carried out. This selection is carried out on the linear definition of deformation components being element reference system independent.

In particular, the proposed approach is based on definitions of only relative lenghts and the finite element construction can be carried out completely in the linear field. In such a way, the analysis is robust because the singularities of rotation matrices are not introduced and we can select the deformative modes that contribute to the expressions of the strain tensor components. In addition, being the mechanical description implicitly conservative, we can note that the analysis is economical because it does not require complex manipulations to overcome the noncommutativity of rotations.

The numerical tests, finally, have shown that low computational time and storage demand are required.

References

[1] Belytschko T., Hsieh B.J., Non-linear transient finite element analysis with convected coordinates, Int. J. Numer. Methods Eng., 1973; **7**; 255-271.

[2] Rankin C.C., Nour-Omid B., The use of projectors to improve finite element performance, Comp. Struct., 1988; **30**; 257-267.

[3] Pacoste C., Co-rotational flat facet triangular elements for shell instability analyses, Comput. Methods Appl. Mech. Engrg., 1998; **156**; 75-110.

[4] Zienkiewicz O.C., Taylor R.L., Too J.M., Reduced integration technique in general analysis af plates and shells, Int. J. Numer. Methods Eng., 1971; **3**; 275-290.

[5] Kosloff D., Frazier G.A., Treatment of hourglass patterns in loworder finite element codes, Int. J. Numer. Anal. Methods Geomech., 1978; **2**; 57-72.

[6] Flanagan D.P.,Belytschko T., A uniform strain hexahedron and quadrilateral with orthogonal hourglass contol, Int. J. Numer. Methods Eng., 1983; **17**; 679-706.

[7] Lopez S., An effective parametrization for asymptotic extrapolations, Comput. Methods Appl. Mech. Engrg., 2000; **189**; 297-311.

[8] Lopez S., Detection of bifurcation points along a curve traced by a continuation method, Int. J. Numer. Methods Eng., 2002; **53**; 983-1004.

[9] Simo J.C., Vu-Quoc L., A three-dimensional finite strain rod model, Part II: Computer aspects, Comput. Methods Appl. Mech. Engrg., 1986; **58**; 79-116.

[10] Cardona A., Huespe A., Evaluation of simple bifurcation points and post-critical path in large finite rotation problems, Comput. Methods Appl. Mech. Engrg., 1999; **175**; 137-156.

[11] Eriksson A., On improved predictions for structural equilibrium path evaluations, Int. J. Numer. Methods Eng., 1993; **36**; 201-220.